[redacted] 4226

[redacted] Life

[redacted] to

[redacted] Aerospace

[redacted] and Haynes 188

[redacted]

[redacted] Arya

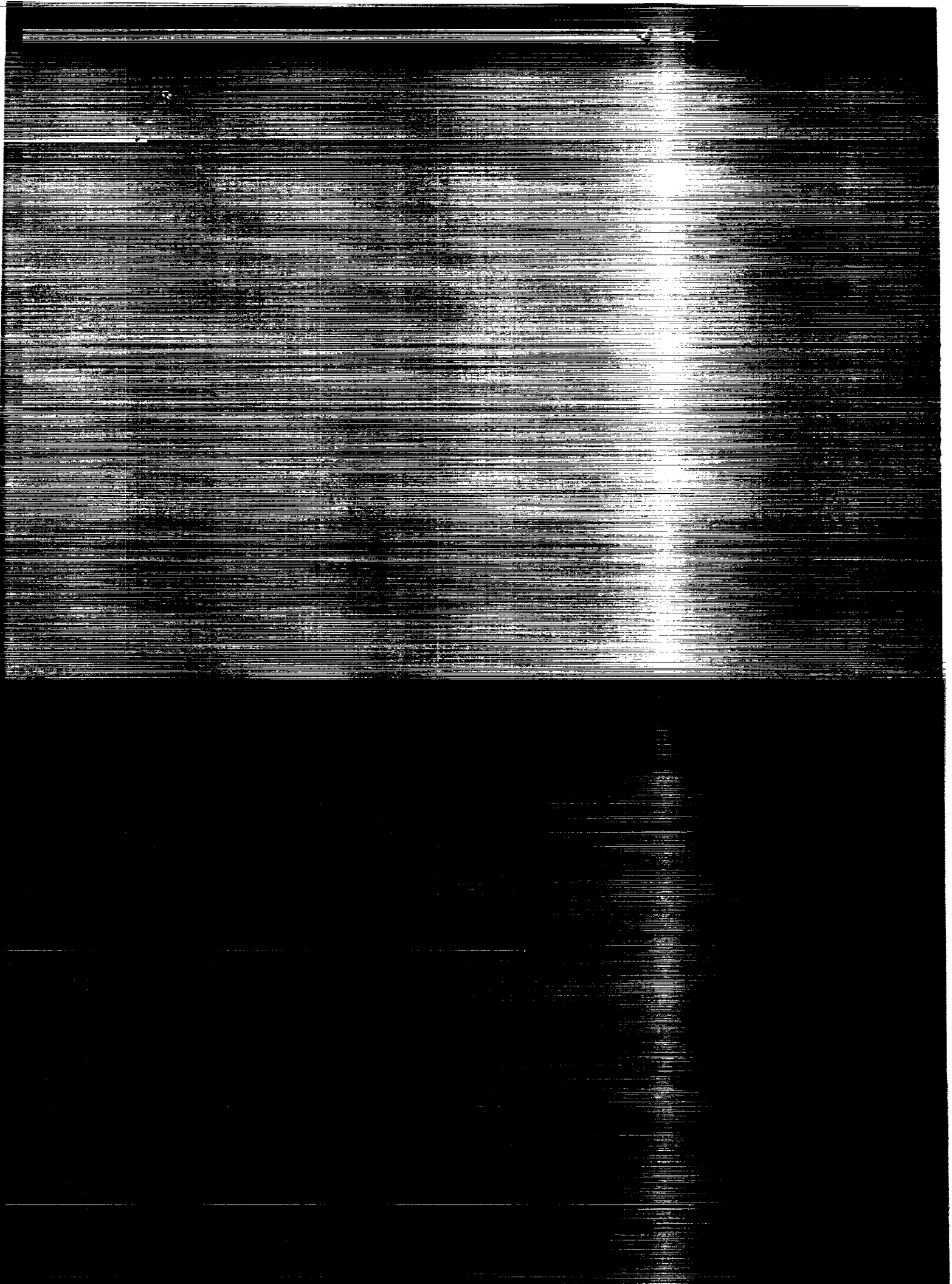

NASA Technical Memorandum 4226

Application of Thermal Life Prediction Model to High-Temperature Aerospace Alloys B1900+Hf and Haynes 188

Gary R. Halford, James F. Saltsman,
Michael J. Verrilli, and Vinod K. Arya
Lewis Research Center
Cleveland, Ohio

NASA
National Aeronautics and
Space Administration
Office of Management
Scientific and Technical
Information Division
1990

Application of Thermal Fatigue Life Prediction Model to High-Temperature Aerospace Alloys B1900+Hf and Haynes 188

Gary R. Halford, James F. Saltsman, and Michael J. Verrilli
National Aeronautics and Space Administration
Lewis Research Center
Cleveland, Ohio 44135

Vinod K. Arya*
University of Toledo
Toledo, Ohio 43606

Summary

This report presents the results of the application of a newly proposed thermomechanical fatigue (TMF) life prediction method to a series of laboratory TMF results on two high-temperature aerospace engine alloys: cast B1900+Hf and wrought Haynes 188. The method, referred to as TMF/TS-SRP, is based on three relatively recent developments: the total strain version of the method of Strainrange Partitioning (TS-SRP), the bithermal testing technique for characterizing TMF behavior, and advanced viscoplastic constitutive models. The high-temperature data reported in a companion publication are used to evaluate the constants in the model and to provide the TMF verification data to check its accuracy. Predicted lives are in agreement with the experimental lives to within a factor of approximately 2.

Introduction

A recently proposed thermal fatigue life prediction method (refs. 1 and 2) is applied here to thermomechanical fatigue (TMF) data generated for two high-temperature superalloys commonly used in the aerospace industry: B1900+Hf and Haynes 188. The principal advantage of the method to engineering design and analysis is the expression of fatigue life in terms of total strainrange, a quantity more readily and accurately assessable than inelastic strainrange or stress alone. The method evolved from the total strain version of the Strainrange Partitioning (TS-SRP) model designed for isothermal low-cycle fatigue life prediction in the low strain regime (refs. 3 to 5). The new method, TMF/TS-SRP, accounts for the influences of thermal fatigue phasing and waveshape by the introduction of calibration data from inphase and out-of-phase bithermal fatigue tests. Phasing and waveshape effects influence TMF behavior in two distinctly different ways through their effect on the flow and failure behavior of a material. Flow behavior refers to both the stress and strain response to imposed cyclic loading and to the elastic strainrange-life relations. Failure behavior refers to the inelastic strainrange-life relations. The elastic and inelastic strainrange-life relations are summed to form the total strainrange-life relation used to predict cyclic life.

Bithermal creep-fatigue cycling experiments (refs. 6 to 8) are used to establish the failure behavior, that is, the inelastic strainrange-life relations, for a zero mean stress condition. Results of these experiments, coupled with advanced cyclic viscoplastic models (refs. 9 to 15), are also used to describe a material's flow behavior, and hence the position of the elastic strainrange versus life curve. Development of mean stresses is also associated with flow behavior, but their influence on cyclic life is a failure behavior. Viscoplastic constitutive modeling is used to assess magnitudes of mean stresses. The effect of mean stress on cyclic life is then determined by using an appropriate mean stress equation. The need to account for mean stress effects applies to all life prediction schemes and is not unique to the method presented here.

Cyclic life is predicted for a specific thermal fatigue cycle by first identifying the nature of that cycle and then constructing the corresponding total strainrange versus cyclic life curve. Each thermal cycle is associated with a unique fatigue curve that can be determined only after details of the particular cycle are specified.

*NASA Resident Research Associate.

Thermomechanical fatigue lives of specimens are predicted for the cast nickel-base alloy B1900+Hf and for the wrought cobalt-base alloy Haynes 188. Details of the thermomechanical fatigue testing program and the experimental results are contained in a companion report (ref. 16).

Symbols

A'	general constant in empirical equations
B	intercept of elastic strainrange-life relations
C	intercept of inelastic strainrange-life relations
C'	intercept of inelastic line for combined creep-fatigue cycles
F	inelastic strain fraction
K	cyclic strain-hardening coefficient
N	number of applied cycles
t	time
Δ	range of variable
ϵ	strain
σ	stress

Subscripts

c	condensed (time)
cc	creep strain in tension, creep strain in compression
cp	creep strain in tension, plastic strain in compression
el	elastic
fm	failure with mean stress
fo	failure with zero mean stress
ij	pp, pc, cp, or cc
in	inelastic
max	maximum
min	minimum
p	plastic strain
pc	plastic strain in tension, creep strain in compression
pp	plastic strain in tension, plastic strain in compression
r	real (time)
t	total

Superscripts

b	power of cyclic life for elastic strainrange-life relations
c	power of cyclic life for inelastic strainrange-life relations
m	general power of time in empirical flow equations
n	cyclic strain-hardening exponent
α	power on total strainrange in empirical flow equations

Background

Engineering methods for predicting thermal fatigue life of materials and structural components, with rare exception (ref. 17), are based on isothermal material behavior. The isothermal temperature may be the maximum, minimum, or mean temperature for which fatigue life is a minimum, or other isothermal temperatures that fall within the operational duty cycle. Such life assessment methods have evolved because of their simplicity and their minimal database requirements. Their shortcomings are becoming more apparent, however, as the demands for improved accuracy of prediction increase.

Micromechanisms of inelastic deformation, cracking, and oxidation kinetics under thermal cycling can be quite different (ref. 18) from those in isothermal fatigue. As a result, lives under thermal cycling can deviate as much as a factor of 10 below corresponding isothermal lives. A key to improved accuracy is the use of a database involving some form of thermal cycling behavior that captures first-order effects without requiring extensive testing. Extensive testing must be avoided since thermal cycling fatigue experiments are quite expensive and time-consuming compared to isothermal testing. In addition, there are many phenomenological parameters to deal with, including maximum temperature, minimum temperature, temperature range, rate of cycling, phase relationship between temperature and mechanical strain, hold times, and so on. Because of the numerous additional variables, a thorough test matrix would become many times larger than required for an isothermal database. What is needed is a framework for dealing with these variables that will significantly reduce the amount of testing required.

The thermomechanical fatigue life prediction approach described here offers such a framework. Although TMF testing is an increased burden when developing the necessary database for a life prediction system, the potential for improving predictive accuracy should offset the added effort for crucial engineering structural components.

There is little justification now for testing and subsequently predicting cyclic life on an isothermal basis. TMF test equipment and techniques have been developed to a point where these tests can be conducted routinely, although they remain complex. Thermal cycling stress-strain hysteresis loops are difficult to analyze and interpret, particularly in the low-strainrange regime where most power-producing equipment operate. A simpler form of thermal and mechanical testing has been developed recently that overcomes these difficulties.

Bithermal fatigue testing (ref. 6) has been proposed as a viable alternative to conventional TMF testing. This testing procedure offers several advantages. First, the tests are easier to conduct and interpret than more conventional TMF testing. In addition, this type of testing captures the first-order effects of alternating temperatures on (a) cyclic stress-strain and creep response, (b) temperature-dependent deformation and crack

initiation mechanisms, and (c) thermal expansion mismatch strains between substrate and internal particles, and between substrate and surface oxides or coatings.

Nearly all life prediction models developed to date have been based on isothermal conditions. This fact, in itself, does not preclude a model from being applied to nonisothermal conditions provided the material-dependent model constants are appropriate for nonisothermal conditions. For example, Strainrange Partitioning (SRP) was first formulated on an isothermal, inelastic strainrange basis (ref. 19). This version has been applied successfully to TMF (ref. 20) at a strain level where the inelastic strainrange can be measured accurately and for which the materials constants in the life relations are insensitive to temperature for the range of temperatures considered. Deformation and cracking mechanisms were identical between thermal and isothermal conditions. Thus, an isothermally based approach was capable of accurately predicting TMF lives because no new mechanisms had been introduced by thermal cycling. This will not be the case in all instances, so this approach cannot be relied on for general TMF life prediction.

Strainrange Partitioning has since been successfully formulated on a total strain basis (TS–SRP), extending it into the isothermal low-strain, long-life regime where the inelastic strains are small and difficult to determine (ref. 5). This extension, plus the introduction of the bithermal test to characterize both TMF failure and flow behavior, has permitted the SRP method to be applied to the general TMF life prediction problem. The method deals with these characteristics independently. Cyclic stress-strain response to imposed mechanical and thermal loading is flow behavior, and it can be represented analytically via cyclic constitutive equations, or experimentally by direct measurements in the laboratory. Failure behavior within the framework of SRP is linked to the relations between cyclic inelastic strains and the cyclic lifetime (i.e., the familiar SRP inelastic strainrange-life relations). Among the advantages of this separation of flow and failure behavior is that the failure behavior constants become less sensitive to major imposed variables such as temperature and time. The strong effects of temperature and time are reflected more in the flow behavior, which can be handled with the aid of highly developed viscoplastic cyclic constitutive models. If a life prediction method has to deal with the significant thermal and temporal influences, the life prediction model and its constants would become quite complex and cumbersome.

Another advantage of the flow-failure behavior distinction lies in the ability to experimentally measure, with only one specimen, the flow behavior of a duty cycle at small strainranges using long times per cycle. These would be prohibitively lengthy and costly experiments to perform to failure wherein several specimens would be required, thus compounding the excessive testing time requirements.

Life Prediction Analysis

The TMF life prediction procedure used herein follows the guidelines set forth in references 2 and 5.

Total Strainrange-Life Relations

Figure 1 shows the total mechanical strainrange $\Delta\epsilon_t$ versus cyclic crack initiation life N_{fo}. This relation, used in the TS–SRP method for isothermal creep-fatigue conditions, has recently been proposed for adaptation for use in TMF life prediction (ref. 2). This report details how that is to be accomplished.

The total strainrange is the sum of two terms: the elastic strainrange $\Delta\epsilon_{el}$ and the inelastic strainrange $\Delta\epsilon_{in}$. Each is a power law function of N_{fo}, and appears as a straight line on the log-log coordinates of figure 1. The equation for the general life relation is shown in the figure and is written as follows:

$$\Delta\epsilon_t = \Delta\epsilon_{el} + \Delta\epsilon_{in} \tag{1a}$$

or

$$\Delta\epsilon_t = B(N_{fo})^b + C'(N_{fo})^c \tag{1b}$$

The subscript o in N_{fo} denotes the fatigue life for an equivalent zero mean stress condition. This is a calculated condition and is discussed later in the section Mean Stress Corrections. Mean stress corrections are made during the conversion of raw laboratory data (with mean stresses) into reduced material property data for equivalent zero mean stress conditions. After applying the material property data to TMF life prediction, the effect of any mean stresses present in the TMF cycles must

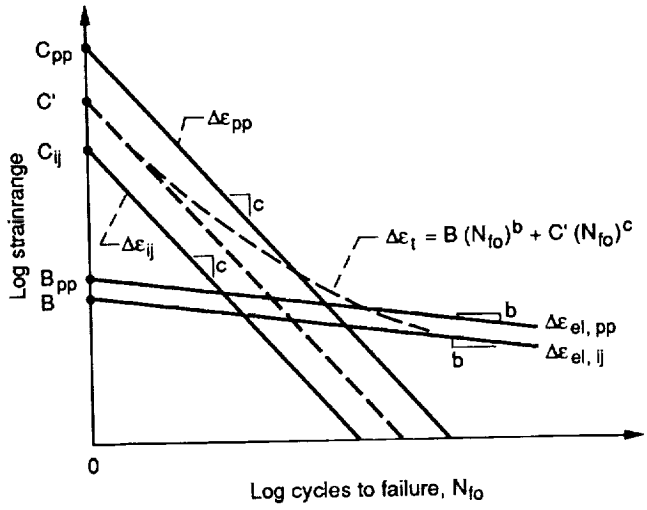

Figure 1.—Strainrange-life relations for total strain version of Strainrange Partitioning (TS–SRP).

be accounted for. The rationale behind the need for mean stress corrections is fully discussed in reference 21.

The objective now is to evaluate exponents b and c, and intercepts B and C' in equation (1) that will be applicable to a broad range of potential thermal and mechanical loading conditions. In general, these four values would be functions of the specific thermal cycling conditions. However, as shown in figure 1, the exponents b and c are fixed; that is, the elastic life relations are shown to be parallel to one another, as are the inelastic life relations. This behavior is supported by observations on the behavior of many materials under a wide range of fatigue conditions (ref. 22). Although it is not a necessary condition for using the TMF/TS-SRP method (see the appendix to ref. 2), parallelism greatly simplifies the algebra of the analysis and aids the reader in following the logic of the method. We will use this simplification here.

The intercepts B and C' in equation (1b) are first-order functions of many of the variables (time, environment, waveshape, temperature, and so on) that are known to influence TMF lives. For example, both B and C' typically decrease as the time per cycle increases (lowered frequency or strain rate, or increased hold time). This is due to the introduction of creep and environmental attack, which are usually regarded as highly detrimental damage mechanisms. As temperature increases, B usually decreases (primarily because of the weakening effect of creep, but also because of environmental attack), and C' may increase or, most likely, decrease. Typically, as more creep deformation is added to a cycle (via higher temperature and/or longer time under stress), the fraction of the inelastic strainrange to total strainrange increases, causing cyclic life to decrease. Further, as creep deformation becomes a greater fraction of the inelastic strainrange, the life also tends to decrease through a drop in the values of both C' and B.

With the simplifying assumption that the slopes are constants, the problem reduces to identifying and quantifying the primary influences on the intercept values. The effects are associated with flow behavior, which can be represented by any one of several recently proposed cyclic constitutive models (refs. 9 to 15). Because of the large number of constants, their interaction, and the lack of physical interpretation, the evaluation of the constants in some of the models can be a difficult task. The constitutive model constants have been determined for B1900+Hf (ref. 10) but not for Haynes 188. Consequently, we have resorted to a simpler empirical model (ref. 4) to represent the cyclic flow behavior of this alloy.

This empirical model was developed from trends exhibited by a more sophisticated isothermal unified constitutive model (ref. 9) with material constants for Hastelloy X. Using this model over a wide range of cyclic conditions has revealed a series of behavior trends that can be described almost as accurately by simpler power law equations (ref. 4). The form of these power law flow equations has been used in representing the Haynes 188 flow response. Examples are provided in the following sections.

Inelastic Strainrange-Life Relations

Let us begin by concentrating on the intercept C' in equation (1b). With the exponent c constant, the algebraic expression for C' is derived from application of the interaction damage rule (ref. 23) of SRP:

$$C' = [\Sigma F_{ij}(C_{ij})^{1/c}]^c \tag{2}$$

where $ij = pp$, pc, cp, or cc and F_{ij} is the inelastic strainrange fraction present in any given TMF cycle, that is, the "partitioning" of the inelastic strainrange $\Delta\epsilon_{in}$. Note that the strain fraction F_{ij} is time, temperature, and waveshape dependent.

$$F_{ij} = \frac{\Delta\epsilon_{ij}}{\Delta\epsilon_{in}} \tag{3a}$$

where

$$\Delta\epsilon_{in} = \Sigma\Delta\epsilon_{ij} \tag{3b}$$

that is,

$$\Sigma F_{ij} = 1 \tag{3c}$$

The values C_{ij} are the strainrange intercepts at one cycle to failure of the SRP inelastic strainrange-life relations,[1]

$$\Delta\epsilon_{in} = C_{ij}(N_{ij})^c \tag{4}$$

In addition to F_{ij}, the other contributors to C' are C_{ij} and c. To predict the lives of inphase or out-of-phase TMF cycles, we need to be concerned only with $\Delta\epsilon_{pp}$ and $\Delta\epsilon_{cp}$ components of inelastic TMF strain for inphase, and pp and pc components for out-of-phase. Bithermal fatigue test results have been reported in a companion report (ref. 16) that provides the database for determining the constants C_{pp}, C_{cp}, C_{pc}, and c. In the process of establishing the "pure" $\Delta\epsilon_{ij}$ inelastic strainrange-life relations for TMF/TS-SRP, the guidelines set forth in reference 28 were used to guarantee sufficient accuracy and significance of computed results. The only departure from

[1]For TMF, there can be two curves for $\Delta\epsilon_{pp}$: one inphase and the other out-of-phase. The $\Delta\epsilon_{cp}$ and $\Delta\epsilon_{pc}$ components of inelastic strainrange are associated with inphase and out-of-phase TMF, respectively. Further, $\Delta\epsilon_{cc}$ is seldom a large strainrange component in TMF, and hence has not been pursued further at this stage of development of the TMF/TS-SRP method. So-called clockwise and counterclockwise "baseball" cycle TMF cycles (ref. 24) may exhibit small components of $\Delta\epsilon_{cc}$. Bithermal testing could be modified to accommodate a $\Delta\epsilon_{cc}$ component if necessary. An additional aspect of the life relations embodied in equation (4) is that the intercepts and slopes, while taken as time independent in this report, can indeed be functions of strain rate or total exposure time (see, for example, refs. 22, and 25 to 27).

the guidelines was the enforcement of a constant value for c for a given material and cycle phase (i.e., equal to the value measured in the $\Delta\epsilon_{pp}$ tests). The pertinent life relations are shown in figure 2 for both alloys. Values of the intercepts and exponents are summarized in table I.

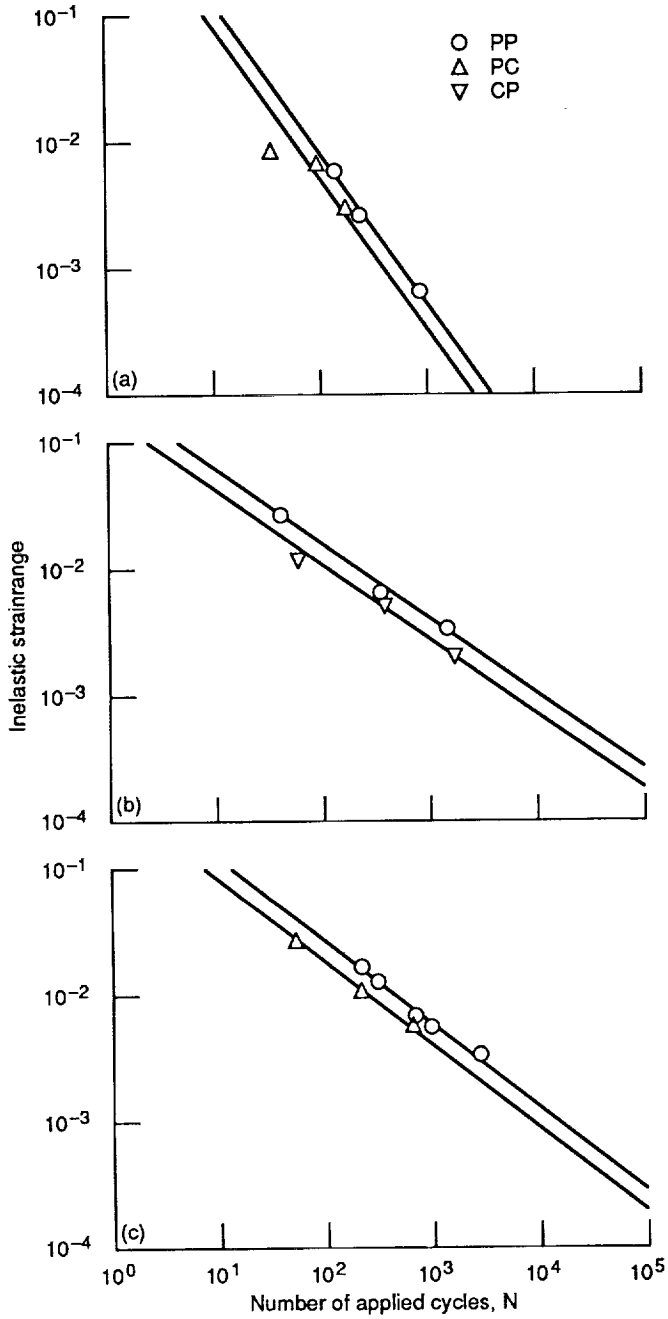

(a) Out-of-phase B1900+Hf, 483↔871 °C.
(b) Inphase Haynes 188, 760↔316 °C.
(c) Out-of-phase Haynes 188, 316↔760 °C.

Figure 2.—Inelastic strainrange-life relations for TMF life prediction (the symbol ↔ denotes thermal cycling: the first value is extreme temperature in tension, the second is extreme temperature in compression).

TABLE I.—FLOW AND FAILURE CONSTANTS FOR TMF/TS-SRP INPHASE AND OUT-OF-PHASE TMF CYCLING

Constant		B1900+Hf (out-of-phase)	Haynes 188	
			Inphase	Out-of-phase
B_{pp}		0.041	0.014	0.016
C_{pp}		1.96	.23	.49
C_{cp}		-----	.16	-----
C_{pc}		1.22	-----	.34
c		−1.19	−.59	−.64
b		−.26	−.12	−.12
b/c		.22	.20	.19
n		.22	.20	.19
A'	Eq. (5)	2.33	.49	.73
α	Eq. (5)	.30	0	.066
m	Eq. (5)	.027	.091	.070
A'	Eq. (8)	.027	.022	.017
α	Eq. (8)	0	0	0
m	Eq. (8)	−.026	−.058	−.041

The next step is to determine, with the aid of equations derived from flow behavior, how the values of F_{ij} vary with time per cycle and with waveshape. (Inphase and out-of-phase TMF continuous strain cycling are of current interest only.) Plasticity is defined as time-independent inelastic deformation, and creep is the time-dependent component. An appropriate unified viscoplastic constitutive model can be used to perform the calculations that permit partitioning of the inelastic strain into these two components. This is done by first computing the stress and inelastic strain versus real time t_r response to an interval of mechanical straining (say, a full cycle) at the strain rate for the TMF control conditions of the problem at hand. By then asking the model to respond to the same stress history applied over a significantly condensed time scale t_c (on the order of less than 1 sec/cycle is usually sufficient, although higher rates could just as easily be applied), we again calculate the inelastic strain response. This calculated inelastic strain response is the time-independent component, that is, the plasticity component. The difference between the originally calculated inelastic strain and the newly calculated plastic strain is simply the time-dependent component which we define as creep. This procedure is shown in figure 3.

Applying this analytic approach to continuous strain cycling TMF cycles, we can deduce the partitioned inelastic strainranges for the duty cycle of interest. If one wishes to investigate the effects on life of variations in total mechanical strainrange or cycle time, additional calculations can be made over a wide range of these values. A correlation between F_{ij}, $\Delta\epsilon_t$, and cycle time t can be established. Plots of F_{ij} versus time per cycle can be represented by straight lines on log-log coordinates. Typically, these lines are parallel with one another

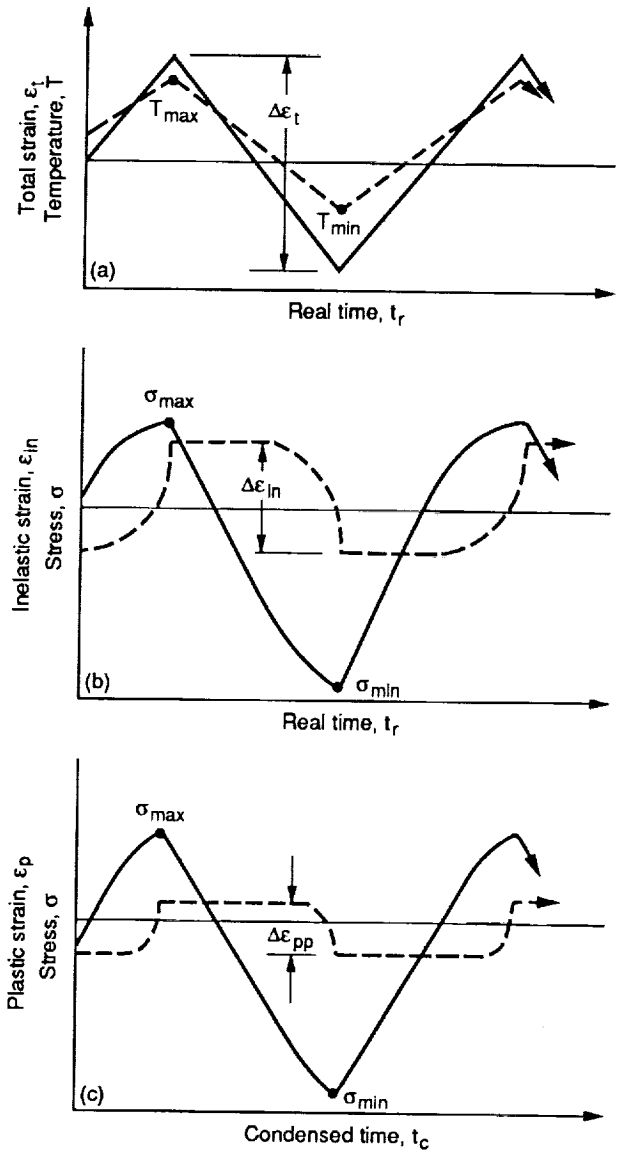

(a) Inphase TMF control conditions in real time.
(b) Stress and inelastic strain response in real time.
(c) Analytically imposed stress and plastic strain response in condensed time.

Figure 3.—Analytic partitioning of inelastic strainrange for inphase TMF cycle, $\Delta\epsilon_{cp} = \Delta\epsilon_{in} - \Delta\epsilon_{pp}$.

according to total strainrange $\Delta\epsilon_t$. Thus, F_{ij} can be written as a power law expression of the time per cycle, normalized by an arbitrary power law function of the total strainrange:

$$F_{ij} = A'(\Delta\epsilon_t)^{\alpha}(t)^{m} \tag{5}$$

The introduction of the $\Delta\epsilon_t$ term is strictly an analytic manipulation of the data that we have found increases the accuracy of the calculations. There is no physical significance to the term or its use. The constants A', α, and m are determined from multiple regression analyses of analytic data.

In equation (5), the variables $\Delta\epsilon_t$ and t are the independent variables, and F_{ij} is the dependent variable.

Multiple regression constants for B1900+Hf were determined in the manner described in the preceding paragraph by using the viscoplastic model of Walker (ref. 10); they are tabulated in table I. When a viscoplastic model is not available, as in the case for Haynes 188, experimental data can be used together with the power law form of equation (5) to represent F_{ij} behavior. When using experimental data, it is important that the test cycle be appropriate to the duty cycle to be predicted. Here we used the inphase and out-of-phase bithermal $\Delta\epsilon_{pp}$, $\Delta\epsilon_{cp}$, and $\Delta\epsilon_{pc}$ test data from reference 16 wherein F_{ij} was measured. Layering of the data according to total strainrange was noted and reduced in the same manner as for the Walker-calculated F_{ij} values for B1900+Hf. Resultant values for A', α, and m for Haynes 188 are also listed in table I.

With the proper constants evaluated from the bithermal fatigue databases on both materials, the position of the TMF inelastic strainrange-life relation can be determined for any inphase or out-of-phase TMF cycle of interest. We must then, however, also determine the proper material constants in the equations that will permit positioning of the elastic strainrange-life relation.

Elastic Strainrange-Life Relations

From reference 16, we know the values of the exponent b of the elastic strainrange-versus-life lines for both alloys, since they were determined from the results of the inphase and out-of-phase bithermal $\Delta\epsilon_{pp}$ experiments. The time-dependent intercept B of the general elastic strainrange-versus-life line is expressed in reference 2 as follows:

$$B = K_{ij}(C')^{n} \tag{6}$$

where n is the cyclic strain hardening exponent,[2] and K_{ij} is a time-dependent cyclic strain hardening coefficient defined by the equation

$$\Delta\epsilon_{el} = K_{ij}(\Delta\epsilon_{in})^{n} \tag{7}$$

The quantities K_{ij} and n are clearly flow characteristics, whereas C' is partially flow and partially failure related. The coefficient K_{ij} is temperature and time dependent as well as waveshape dependent. These dependencies are embodied in viscoplasticity models. The Walker model (ref. 10) was used to determine K_{ij} values for B1900+Hf for a wide range of

[2]The exponent n is related to b and c by the expression $n = b/c$. Since b and c are independent of the major cycle variables, n is also considered to be a constant for a given material. For purposes of consistency in life calculation, the value of b/c will be used instead of n as determined by a regression analysis of the relevant test data.

total strainranges and cycle times for the continuous triangular strain and temperature thermomechanical out-of-phase cycle. Plots of K_{ij} versus cycle time revealed trends similar to those found for plots of F_{ij} versus cycle time except that the data could be represented by a single log-log linear line given by the equation

$$K_{ij} = A'(t)^m \tag{8}$$

Table I contains values of A' and m for representing K_{ij} for out-of-phase TMF cycles of B1900+Hf, and for both inphase and out-of-phase TMF cycles of Haynes 188. Least-squares curve fit constants were determined for equation (8) by using the experimental bithermal data for Haynes 188 (ref. 16). Normally, it would be preferred that a viscoplastic model, rather than approximate bithermal information, be used to ascertain the values of the constants in equation (8), but model constants are not as yet available for this alloy. Note that the temperature dependency of K_{ij} for Haynes 188 did not have to be addressed, since the extreme temperatures for the bithermal and the TMF tests were selected to be identical. Sufficient flow and failure information has now been assembled to predict TMF lives for a zero mean stress condition N_{f_0}.

Mean Stress Corrections

As a general rule in thermal fatigue, mean stresses are present; consequently, a mean stress correction should be applied to N_{f_0} to permit calculation of the TMF lives. For the present TMF data, the mean stress corrections to life were found to be insignificant (on the order of 1 percent or less), mainly because of the relatively large inelastic strainranges. As a result, corrections were not applied to the data reported herein. See reference 2 for procedures to follow when mean stress effects are large enough to merit attention.

TMF Life Prediction

Table I lists the constants needed to perform the life prediction calculations for the TMF tests reported in reference 16. Shown in table II are the observed and predicted lives. To illustrate the problem of TMF life prediction by the TMF/TS-SRP method, we have selected an out-of-phase TMF test of B1900+Hf with a total mechanical strainrange of 0.0072. The appropriate total mechanical strainrange versus life curve (for equivalent zero mean stress condition) is shown in figure 4. With a total strainrange of 0.0072, a resultant life N_{f_0} was determined to be 491 cycles to failure, compared with the observed life of 546.

Predicted and observed lives for all TMF tests are compared in figure 5. Agreement is generally within the conventional factor of 2 associated with high-temperature fatigue life prediction in the nominally low-cycle fatigue regime. It should be noted that the test cycles that were predicted were not used to establish any of the correlations used to make the predictions.

TABLE II.—RESULTS OF LIFE PREDICTION CALCULATIONS OF CONTINUOUS-CYCLING STRAIN-TEMPERATURE THERMOMECHANICAL FATIGUE CYCLES

[The symbol ↔ denotes thermal cycling: the first value is extreme temperature in tension; the second is extreme temperature in compression.]

Total mechanical strainrange, $\Delta\epsilon_t$, percent	Observed life, N_{f_0}, cycles	Inelastic strain fraction, F_{pp}	Predicted life, N_{f_0}, cycles	Predicted N_{f_0}/ observed N_{f_0}
Out-of-phase B1900+Hf ($\Delta\epsilon_{pc} + \Delta\epsilon_{pp}$), 483↔871 °C				
3.22	16	0.04	31	1.94
1.47	55	.24	99	1.80
1.38	67	.25	111	1.66
1.05	124	.31	189	1.52
.72	546	.38	491	.90
.47	1992	.45	2178	1.09
Inphase Haynes 188 ($\Delta\epsilon_{cp} + \Delta\epsilon_{pp}$), 760↔316 °C				
3.51	28	0.27	23	0.82
2.90	39	.27	35	.90
1.16	829	.27	339	.41
Out-of-phase Haynes 188 ($\Delta\epsilon_{pc} + \Delta\epsilon_{pp}$), 316↔760 °C				
2.46	191	0.22	106	0.56
1.36	477	.25	387	.81
.83	720	.27	1390	1.93

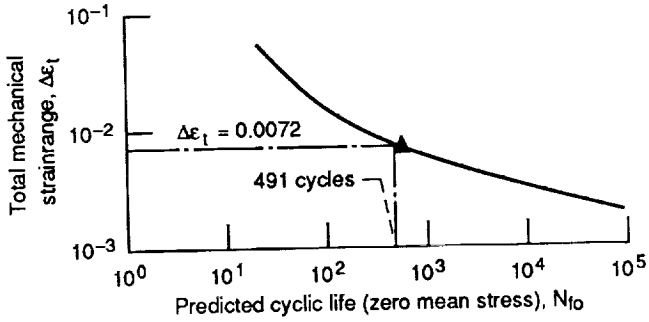

Figure 4.—Example TMF/TS-SRP life prediction curve (zero mean stress condition) constructed for B1900+Hf (out-of-phase; 483↔871 °C; 4 min/cycle; total strainrange $\Delta\epsilon_t$, 0.0072; observed life, 546 cycles; predicted life, 491 cycles).

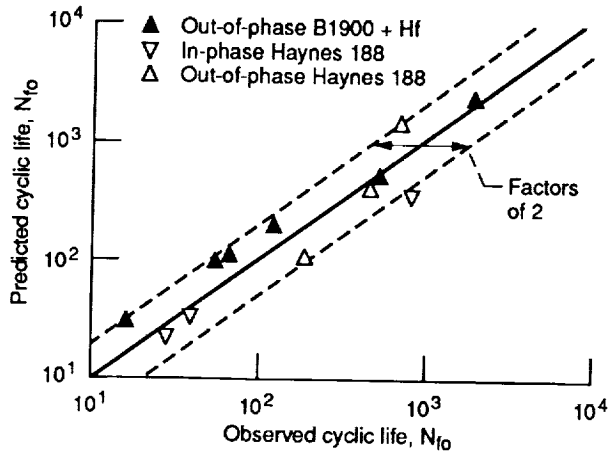

Figure 5.—Assessment of TMF life prediction capability of TMF/TS-SRP method for B1900+Hf and Haynes 188.

Discussion and Concluding Remarks

The driving force for developing the current TMF/TS-SRP life prediction approach is the need for such a model in the low-strainrange, nominally elastic regime where most power-producing equipment operates. Attempts to calculate inelastic strainranges would be fruitless, since the accuracy would likely be unacceptable. In addition, generation of high-quality life prediction "calibration" data is prohibitively expensive because of the excessively long testing times and the requirement of sophisticated and expensive computer-controlled servo test equipment. A life prediction model that can be extrapolated with confidence into this analytically and experimentally difficult regime is highly sought after. We have presented the framework for what is felt to be a life prediction method that meets these requirements.

The only input information required of the TMF tests for which life was predicted by the TMF/TS-SRP method was the total mechanical strainrange, the maximum and minimum temperatures, the TMF cycle waveshape, and the time per cycle. Considerably more information was needed to obtain the characteristics of the materials involved. However, once that information has been documented, it can be applied to the life prediction of a wide range of TMF problems.

An extremely important aspect of the life prediction method is that at no time was it necessary to measure or even calculate the magnitude of the inelastic strainrange of the TMF cycles. Calculations were made of quantities that could be used in the calculation of $\Delta\epsilon_{in}$, but they were not needed for the TMF life prediction. The accuracy that has been demonstrated in the current case is adequate based on the standard of factors of ± 2 deviation in cyclic life. The reasonable success of the TMF/TS-SRP life predictions is attributed to the fact that the primary life prediction variable is the total strainrange. An interesting point is that the errors in the constituent inelastic and elastic components of strainrange are of a compensating nature. That is, if the elastic strainrange was calculated to be too large (implying short life), it would have implied a much smaller inelastic strainrange (implying long life). Similarly, too large an inelastic strainrange would be offset by an implied abnormally low elastic strainrange. The nature of the compensating errors provides numerical stability to this total strainrange life prediction model.

Obviously a considerable amount of other material information, as measured, for example, from bithermal flow and failure tests, was required to permit the desired life prediction calculations. These data have been reported in reference 16, and have been reduced to equation form with appropriate constants recorded in this report. The current TMF tests had a maximum life of only 2000 cycles to failure. A need still exists for a verification data base in the longer life range of 5000 to 50 000 cycles to failure.

The actual calculation of TMF life is a trivial exercise once the total strainrange versus cyclic life failure curve has been established for the specific conditions of the cycle of interest.

References

1. Halford, G.R.; and Saltsman, J.F.: Total Strain Version of Strainrange Partitioning for Thermomechanical Fatigue at Low Strains. Turbine Engine Hot Section Technology. NASA CP-2493, 1987, pp. 435-458.
2. Saltsman, J.F.; and Halford, G.R.: Life Prediction of Thermomechanical Fatigue Using The Total Strain Version of Strainrange Partitioning (SRP)—A Proposal. NASA TP-2779, 1988.
3. Halford, G.R.; and Saltsman, J.F.: Strainrange Partitioning—A Total Strain Range Version. Advances in Life Prediction Methods, D.A. Woodford and J.R. Whitehead, eds., American Society of Mechanical Engineers, 1983, pp. 17-26.
4. Saltsman, J.F.; and Halford, G.R.: An Update of the Total-Strain Version of Strainrange Partitioning. Low Cycle Fatigue, ASTM STP-942, H.D. Solomon, et al., eds., American Society for Testing and Materials, Philadelphia, 1988, pp. 329-341.
5. Saltsman, J.F.; and Halford, G.R.: Procedures for Characterizing an Alloy and Predicting Cyclic Life With the Total Strain Version of Strainrange Partitioning. NASA TM-4102, 1989.
6. Halford, G.R., et al.: Bithermal Fatigue—A Link Between Isothermal and Thermomechanical Fatigue. Low Cycle Fatigue, ASTM STP-942, H.D. Solomon, et al., eds., American Society for Testing and Materials, Philadelphia, 1988, pp. 625-637.
7. Gayda, J., et al.: Bithermal Low-Cycle Fatigue Behavior of a NiCoCrAlY-Coated Single-Crystal Superalloy. Effects of Load and Thermal Histories on Mechanical Behavior of Materials, P.K. Liaw and T. Nicholas, eds., The Metallurgical Society of AIME, New York, 1987, pp. 179-198.
8. Verrilli, M.J.: Bithermal Fatigue of a Nickel-Base Superalloy Single Crystal. NASA TM-100885, 1988.
9. Walker, K.P.: Research and Development Program for Non-Linear Structural Modeling With Advanced Time-Temperature Dependent Constitutive Relationships. (PWA-5700-50, Pratt and Whitney Aircraft; NASA Contract NAS3-22055), NASA CR-165533, 1981.
10. Chan, K.S., et al.: High Temperature Inelastic Deformation Under Uniaxial Loading: Theory and Experiment. J. Eng. Mater. Technol., vol. 111, no. 4, Oct. 1989, pp. 345-353.
11. Bodner, S.R.; and Partom, Y.: Constitutive Equations for Elastic-Viscoplastic Strain-Hardening Materials. J. Appl. Mech., vol. 42, no. 2, June 1975, pp. 385-389.

12. Bodner, S.R.: Review of a Unified Elastic-Viscoplastic Theory. Unified Constitutive Equations for Creep and Plasticity, A.K. Miller, ed., Elsevier Applied Science Publishers, 1987, pp. 273-301.
13. Miller, A.K.: An Inelastic Constitutive Model for Monotonic Cyclic, and Creep Deformation, Parts 1 and 2. J. Eng. Mater. Technol., vol. 98, no. 2, Apr. 1976, pp. 97-113.
14. Robinson, D.A.; and Swindeman, R.W.: Unified Creep-Plasticity Constitutive Equations for 2-1/4Cr-1Mo Steel at Elevated Temperature. ORNL TM-8444, Oak Ridge National Laboratories, Oak Ridge, TN, 1982.
15. Freed, A.D.: Thermoviscoplastic Model With Application to Copper. NASA TP-2845, 1988.
16. Halford, G.R., et al.: Thermomechanical and Bithermal Fatigue Behavior of Cast B1900+Hf and Wrought Haynes 188. NASA TM-4225, 1990. (Submitted to the ASTM for inclusion in the Special Technical Publication of the First Symposium on Advances in Fatigue Lifetime Prediction Techniques, Apr. 1990, San Francisco, CA.)
17. Polhemus, J.F.; Spaeth, C.E.; and Vogel, W.H.: Ductility Exhaustion Model for Prediction of Thermal Fatigue and Creep Interaction. Fatigue at Elevated Temperatures, ASTM STP-520, A.E. Carden, A.J. McEvily, and C.H. Wells, eds., American Society for Testing and Materials, Philadelphia, PA, 1973, pp. 625-636.
18. Halford, G.R.: Low Cycle Thermal Fatigue. Thermal Stresses II, R.B. Hetnarski, ed., Elsevier Science Publishers, Amsterdam, 1987, pp. 329-428.
19. Manson, S.S.; Halford, G.R.; and Hirschberg, M.H.: Creep-Fatigue Analysis by Strain-Range Partitioning, Design for Elevated Temperature Environments, S.Y. Zamrik, ed., ASME, 1971, pp. 12-28.
20. Halford, G.R.; and Manson, S.S.: Life Prediction of Thermal-Mechanical Fatigue Using Strainrange Partitioning. Thermal Fatigue of Materials and Components, ASTM STP-612, D.A. Spera and D.F. Mowbray, eds., American Society for Testing and Materials, Philadelphia, 1976, pp. 239-254.
21. Halford, G.R.; and Nachtigall, A.J.: Strainrange Partitioning Behavior of an Advanced Gas Turbine Disk Alloy AF2-1DA. J. Aircraft, vol. 17, no. 8, Aug. 1980, pp. 598-604.
22. Halford, G.R.; Saltsman, J.F.; and Hirschberg, M.H.: Ductility Normalized Strain-Range Partitioning Life Relations for Creep-Fatigue Life Predictions. Environmental Degradation of Engineering Materials, M.R. Louthan, Jr. and R.P. McNitt, eds., Virginia Polytechnic Institute, Blacksburg, VA, 1977, pp. 599-612.
23. Manson, S.S.: The Challenge to Unify Treatment of High Temperature Fatigue—A Partisan Proposal Based on Strainrange Partitioning. Fatigue at Elevated Temperatures, ASTM STP-520, American Society for Testing and Materials, Philadelphia, 1973, pp. 744-782.
24. Nelson, R.S.; Schoendorf, J.F.; and Lin, L.S.: Creep Fatigue Life Prediction for Engine Hot Section Materials (Isotropic). NASA CR-179550, 1986.
25. Saltsman, J.F.; and Halford, G.R.: Strainrange Partitioning Life Predictions of the Long Time Metal Properties Council Creep-Fatigue Tests. Methods for Predicting Material Life in Fatigue, W.J. Ostergren and J.R. Whitehead, eds., American Society of Mechanical Engineers, 1979, pp. 101-132.
26. Kalluri, S.; Manson, S.S.; and Halford, G.R.: Exposure Time Considerations in High Temperature Low Cycle Fatigue. Mechanical Behavior of Materials-5, Vol. 2, M.G. Yan, S.H. Zhang, and Z.M. Zheng, eds., Pergamon Press, 1987, pp. 1029-1036.
27. Kalluri, S.; Manson, S.S.; and Halford, G.R.: Environmental Degradation of 316 Stainless Steel in High Temperature Low Cycle Fatigue. Third International Conference on Environmental Degradation of Engineering Materials, M.R. Louthan, Jr. and R.P. McNitt, eds., The Pennsylvania State University, University Park, PA, 1987, pp. 503-519.
28. Hirschberg, M.H.; and Halford, G.R.: Use of Strainrange Partitioning to Predict High-Temperature Low-Cycle Fatigue Life. NASA TN D-8072, 1976.

NASA
National Aeronautics and Space Administration

Report Documentation Page

1. Report No.	2. Government Accession No.	3. Recipient's Catalog No.
NASA TM-4226		

4. Title and Subtitle

Application of Thermal Life Prediction Model to High-Temperature Aerospace Alloys B1900+Hf and Haynes 188

5. Report Date

December 1990

6. Performing Organization Code

7. Author(s)

Gary R. Halford, James F. Saltsman, Michael J. Verrilli, and Vinod K. Arya

8. Performing Organization Report No.

E-5511

10. Work Unit No.

505-63-1B

9. Performing Organization Name and Address

National Aeronautics and Space Administration
Lewis Research Center
Cleveland, Ohio 44135-3191

11. Contract or Grant No.

13. Type of Report and Period Covered

Technical Memorandum

12. Sponsoring Agency Name and Address

National Aeronautics and Space Administration
Washington, D.C. 20546-0001

14. Sponsoring Agency Code

15. Supplementary Notes

Gary R. Halford, James F. Saltsman, and Michael J. Verrilli, NASA Lewis Research Center. Vinod K. Arya, NASA Resident Research Associate and University of Toledo, Toledo, Ohio 43606.

16. Abstract

This report presents the results of the application of a newly proposed thermomechanical fatigue (TMF) life prediction method to a series of laboratory TMF results on two high-temperature aerospace engine alloys. The method, referred to as TMF/TS-SRP, is based on three relatively recent developments: the total strain version of the method of Strainrange Partitioning (TS-SRP), the bithermal testing technique for characterizing TMF behavior, and advanced viscoplastic constitutive models. The high-temperature data reported in a companion publication are used to evaluate the constants in the model and to provide the TMF verification data to check its accuracy. Predicted lives are in agreement with the experimental lives to within a factor of approximately 2.

17. Key Words (Suggested by Author(s))	18. Distribution Statement
Fatigue (metal); Thermal fatigue; Thermomechanical fatigue; Bithermal fatigue; Creep-fatigue; Low-cycle fatigue; High-temperature fatigue; Life prediction; Structural durability; Flow behavior	Unclassified – Unlimited Subject Category 39

19. Security Classif. (of this report)	20. Security Classif. (of this page)	21. No. of pages	22. Price*
Unclassified	Unclassified	12	A03

NASA FORM 1626 OCT 86

*For sale by the National Technical Information Service, Springfield, Virginia 22161

NASA-Langley, 1990